Supplementary material for 'Location retrieval using qualitative place signatures of visible landmarks'

Lijun Wei[a], Valérie Gouet-Brunet[b], and Anthony G. Cohn[a, c, d]

[a]School of Computing, University of Leeds, UK
[b]LaSTIG, IGN-ENSG, Gustave Eiffel University, France
[c]Department of Computer Science and Technology, Tongji University, Shanghai, China
[d]The Alan Turing Institute, United Kingdom

ARTICLE HISTORY
Compiled April 26, 2024

This document provides the supplementary material to the manuscript 'Location retrieval using qualitative place signatures of visible landmarks' accepted for publication by the 'International Journal of Geographical Information Science' with DOI: https://doi.org/10.1080/13658816.2024.2348736. It should be read in conjunction with the main manuscript.

Appendices

A. *Links to websites and datasets mentioned in the main text*

For all websites and datasets mentioned in the main text, their links are listed below based on order of appearance and the last accessed date is 2024-04-26.

- UK Ordnance Survey Roadside Asset Data Services: https://osonline.maps.arcgis.com/apps/View/index.html?appid=61436bfcb44e4acaa99014a8f723e0e5.
- Find Open Data: https://data.gov.uk/.
- OpenDataParis: http://opendata.paris.fr.
- OpenStreetMap: https://www.openstreetmap.org.
- Street lights: https://data.gov.uk/dataset/3bcfdacd-705c-4370-a60a-64e17a1c9e03/street-lights-unmetered.
- Traffic signals: https://data.gov.uk/dataset/12c387e1-e65f-4d9e-a576-05dbc8f1d038/traffic-signals-in-leeds.
- Bins: https://data.gov.uk/dataset/adb73cd0-08ee-4963-b3a1-6f3066fcce0c/litter-bin-locations.
- Trees : https://data.gov.uk/dataset/d8fc56a4-4e57-4e22-b202-eff063545f72/trees-in-leeds-city-centre.
- Bus stops: https://datamillnorth.org/dataset/west-yorkshire-bus-stops.
- Traffic light crossing points: https://data.gov.uk/dataset/b1a820fe-6aff-404f-85cd-ff3484142040/pedestrian-crossing-points.
- War memorials: https://data.gov.uk/dataset/c99488fb-6244-4b84-8345-b7fda39bbd28/war-memorials.
- Bike parking bays : https://data.gov.uk/dataset/de5bc73e-ad4a-4282-b74a-a762204dad4f/leeds-city-centre-bike-bays.

CONTACT Lijun Wei. Author. Email: villager5whu@gmail.com

- Public convenience/toilets: https://data.gov.uk/dataset/dee4f4dd-bea7-43c2-b6b4-098f7b91396b/public-toilets.
- Ordnance survey *OS OpenMap - Local*: https://osdatahub.os.uk/downloads/open/OpenMapLocal.

B. *An illustration of the method proposed by Schlieder, (1993)*

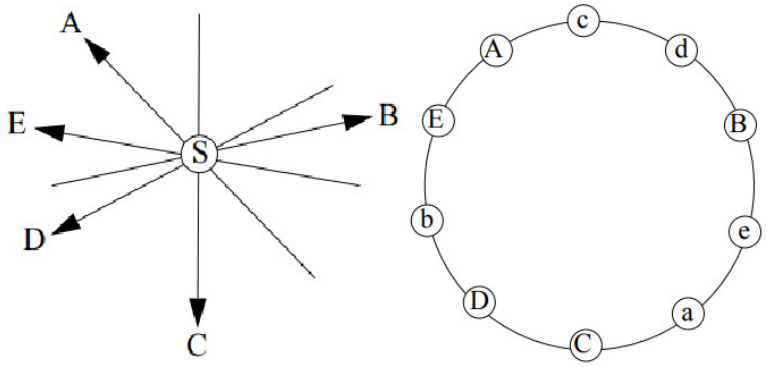

Figure 1. Given a location S and five co-visible landmarks {ABCDE}, the panorama proposed by Schlieder, (1993) can be written as $\langle AcdBeaCDbE \rangle$ where the lower case letters represent the complementary (180^o) directions w.r.t. the landmarks A, B, C, D, E.

Reference: Schlieder, C., 1993. Representing visible locations for qualitative navigation. *Qualitative Reasoning and Decision Technologies*, 523–532.

C. *Algorithm to remove the visibility area occluded by buildings*

Given the visibility zone of a landmark as a polygon stored in *geom* (after removing areas directly in buildings), and the *centre* of the landmark, the visibility area occluded by building can be calculated as given in Algorithm 1:

D. *The uncertainty of perception on landmarks and spatial relations*

D.1. Defining the likelihood of landmarks perception errors

The likelihood of a landmark being incorrectly perceived (e.g. deleted/missed due to occlusion) may vary between different types of landmarks when other conditions are the same. For example, compared with road signs, city trees are generally less likely to be occluded by vehicles as they are usually taller and wider. Other than the impact w_1^n of the visual attributes of landmarks (as discussed in Section 4.2 of the main manuscript), such as landmark **height, width/size, visual salience**, two additional factors can be considered:

(1) w_1^n**: weight of node change cost based on landmark visual attributes**. In general, this likelihood of deletion, insertion and substitution changes could be related to the **height, width/size, visual salience** of landmarks, as well as their **closeness to the viewer**. The bigger a landmark is on the viewer's retina or a camera's image plane (which means taller, bigger or closer) and more salient it is (depending on factors like colour, pattern, static/flashing etc.), the less likely a landmark will be deleted/missed or substituted (e.g. being identified

Algorithm 1 Remove visibility areas behind any buildings

```
procedure MB_VISIBILITY(geom, center)
    rMax := max(dist(center, points)) for all points on the visibility zone geom
    ring := ST_Dump(Boundary(geom))
    for k = 1 : size(ring) − 1 do                    ▷ loop over all edges on boundary
        p:=ring(k); q:=ring(k+1)
        dp:=dist(center,p); dq:=dist(center,q)
        if dp=0 Or dq=0 then
            Continue
        end if
        dp := 2*rMax/dp; dq := 2*rMax/dq
        p2.x := p.x+dp*(p.x-center.x); p2.y := p.y+dp*(p.y-center.y)
        q2.x := q.x+dq*(q.x-center.x); q2.y := q.y+dq*(q.y-center.y)
        occluder := Polygon([p,q,q2,p2,p])
        res := st_diff(geom, occluder)
    end for
    return res
end procedure
```

as other types of landmarks), thus the higher the (weight of) change cost will be. This relation could be expressed as:

(2) w_2^n**: weight of the substitution cost in landmarks perception based on the detailed level of landmark semantics**. In addition to the general 'type' of a landmark, a levelled representation strategy T—sT—n can be used to further enrich their semantic information by combining their general type (T), e.g. 'shop'), sub-type (ST, e.g. 'restaurant', 'laundry'), and name (n) if there are any. As it is generally easier for a human to get the more general information correct than the details, for example, it is easier to identify a *bin* than providing its exact *material*, the (weight of) the cost of the change of more general information would be higher than more detailed information. The total substitution cost ccan be updated as:

$$C^{subst} = w_2^{n,1} C_{node}^{type} + w_2^{n,2} cost_{sub\_type} + w_2^{n,3} cost_{name} \tag{1}$$

For example, if we set $w_2^{n,1} = 0.6, w_2^{n,2} = 0.3, w_2^{n,3} = 0.1$, the total substitution costs between the eight observed landmarks shown in Table 2 and the reference $\{T$—ST—$N\}$ are listed. The smaller the substitution cost is, the more similar two landmarks will be.

(3) w_3^n**: weight of the change cost based on the closeness of landmarks to the viewer.** While the difference brought in by the **height, size and visual salience** attributes can be roughly predefined using the above strategy, the difference brought in by the closeness of landmarks to a viewer is location-dependent. When a viewer is closer to a landmark, there should be less chance for the landmark to be incorrectly perceived, therefore with a higher cost of change. Note that there is no need for a viewer to provide the distance information. By assessing the location of landmarks and the centroids of place cells, a weight w_3^n can be assigned to the change cost of each landmark, which is inversely proportional to the distance between a landmark and a viewer as, written

Table A.1. The composition table of *IOC* relations.

	$\mathrm{Br_2C}$										
$\mathbf{Ar_1B}$	p	m	o^+	o^-	si^+	si^-	di^+	di^-	fi^+	fi^-	c^+
p	p	p	p	p	p	p	p	p	p	p	p
m	p	p	p	p	m	m	p	p	p	p	m
o^+	p	p	p m o^+	p m $o^{+,-}$	di^+ fi^+ o^+	$di^{+,-}$ $fi^{+,-}$ $o^{+,-}$	p m di^+ fi^+ o^+	p m $di^{+,-}$ $fi^{+,-}$ $o^{+,-}$	p m o^+	p m $o^{+,-}$	o^+
o^-	p	p	p m $o^{+,-}$	p m o^-	$di^{+,-}$ $fi^{+,-}$ $o^{+,-}$	di^- fi^- o^-	p m $di^{+,-}$ $fi^{+,-}$ $o^{+,-}$	p m di^- fi^- o^-	p m $o^{+,-}$	p m o^-	$o^{+,-}$
si^+	p m $di^{+,-}$ $fi^{+,-}$ $o^{+,-}$	$di^{+,-}$ $fi^{+,-}$ $o^{+,-}$	di^+ fi^+ o^+	$di^{+,-}$ $fi^{+,-}$ $o^{+,-}$	si^+	$si^{+,-}$	di^+	$di^{+,-}$	di^+	$di^{+,-}$	si^+
si^-	p m $di^{+,-}$ $fi^{+,-}$ $o^{+,-}$	$di^{+,-}$ $fi^{+,-}$ $o^{+,-}$	$di^{+,-}$ $fi^{+,-}$ $o^{+,-}$	di^- fi^- o^-	$si^{+,-}$	si^-	$di^{+,-}$	di^-	$di^{+,-}$	di^-	$si^{+,-}$
di^+	p m di^+ fi^+ o^+	di^+ fi^+ o^+	di^+ fi^+ o^+	$di^{+,-}$ $fi^{+,-}$ $o^{+,-}$	di^+	$di^{+,-}$	di^+	$di^{+,-}$	di^+	$di^{+,-}$	di^+
di^-	p m $di^{+,-}$ $fi^{+,-}$ $o^{+,-}$	$di^{+,-}$ $fi^{+,-}$ $o^{+,-}$	$di^{+,-}$ $fi^{+,-}$ $o^{+,-}$	di^- fi^- o^-	$di^{+,-}$	di^-	$di^{+,-}$	di^-	$di^{+,-}$	di^-	$di^{+,-}$
fi^+	p	m	o^+	$o^{+,-}$	di^+	$di^{+,-}$	di^+	$di^{+,-}$	fi^+	$fi^{+,-}$	fi^+
fi^-	p	m	$o^{+,-}$	o^-	$di^{+,-}$	di^-	$di^{+,-}$	di^-	$fi^{+,-}$	fi^-	$fi^{+,-}$
c^+	p	m	o^+	$o^{+,-}$	si^+	$si^{+,-}$	di^+	$di^{+,-}$	fi^+	$fi^{+,-}$	c^+

as $w_3^n \propto \frac{1}{distance(viewer,landmark)}$. As a maximum visible range D_{max}^i was predefined for each type of landmarks (i = signs, traffic lights, etc.), the corresponding

Table B.1. Example oft the landmark substitution cost w.r.t. a reference landmark L: $\langle T|ST|N\rangle$. The smaller the substitution cost is, the more similar two landmarks will be.

Observation	Non-weighted cost	Weighted substitution cost
$T_2\|ST_2\|N_2$	$1+1+1=3$	$0.6+0.3+0.1=1$
$T_2\|ST_2\|N$	$1+1+0=2$	$0.6+0.3+0.1*0=0.9$
$T_2\|ST\|N_2$	$1+0+1=2$	$0.6+0.3*0+0.1=0.7$
$T_2\|ST\|N$	$1+0+0=1$	$0.6+0.3*0+0.1*0=0.6$
$T\|ST_2\|N_2$	$0+1+1=2$	$0.6*0+0.3+0.1=0.4$
$T\|ST_2\|N$	$0+1+0=1$	$0.6*0+0.3+0.1*0=0.3$
$T\|ST\|N_2$	$0+0+1=1$	$0.6*0+0.3*0+0.1=0.1$
$T\|ST\|N$	$0+0+0=0$	$0.6*0+0.3*0+0.1*0=0$

weighting value w_3^n can be defined as:

$$w_3^n \propto \frac{D^i_{max} - D^i}{D^i_{max}} \tag{2}$$

where a small D^i means that the location is close to the landmark, thus it should be very unlikely for the landmark to be incorrectly perceived ($w_3^n \approx 1$); while a D^i close to D_{max} means that the locations is near the boundary of the visibility range of the landmark, thus more likely to be incorrectly perceived ($w_3^n \approx 0$). We could also impose a tiny weight in this case.

D.2. Defining the likelihood of perception errors on spatial relations

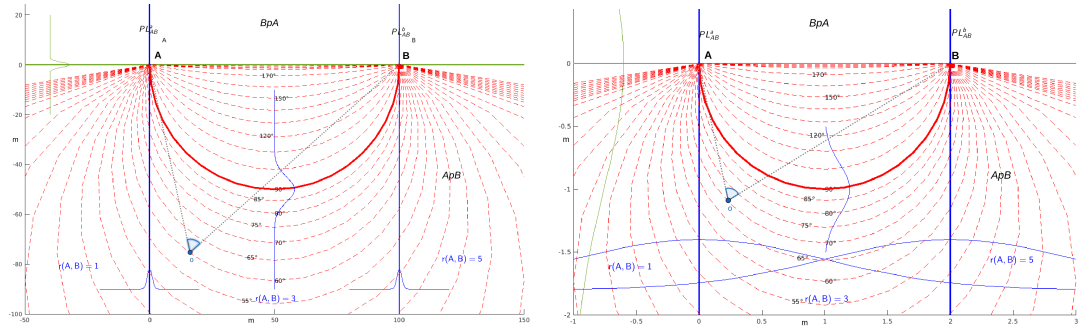

(a) The likelihood of edge perception errors for two 100-metres apart landmarks A, B.

(b) The likelihood of edge perception errors for two two-metres apart landmarks A, B.

Figure B.1. The likelihood of perception errors on the ordering relation, relative orientations and qualitative angles are approximated as Gaussian distributions w.r.t. the distance to the corresponding dividing line or the angular difference to 90°. Note the plotted probability density functions in the figures are only shown for illustration purpose.

As discussed earlier in Section 3 of the main manuscript, three types of lines between each pair of co-visible landmarks are used to divide the space into place cells such that the corresponding type of spatial relations can be consistently observed in each cell, including *Straight Line* for *ordering relation*, *Perpendicular Line* for *relative orientations* and *Circular Line* for *relative angles*. As shown in Figure B.1, when a viewer is approaching either of these dividing lines, they would be less confident in

their judgement of the corresponding spatial relation being observed. The more uncertain this observation is, the more likely the observation could be different from those stored in the reference database, thus the lower the (weight of the) change cost of this relation would be.

More specifically, we can model these uncertainties as independent Gaussian distributions w.r.t. the viewer's distance to the corresponding dividing line or the angular difference to 90^o. The three probability density functions of *ordering relation*, *relative orientation* and *qualitative angle* at a location o can be written as:

$$f(o)_1 = \frac{1}{\sigma_1\sqrt{2\pi}}\exp^{-\frac{1}{2}\left(\frac{d(o,\overleftrightarrow{AB})}{\sigma_1}\right)^2} \tag{3}$$

where $d(o, \overleftrightarrow{AB})$ is the distance between a location o and line $\overleftrightarrow{AB}$. When viewers are between the two perpendicular lines, i.e. *relative orientation* index $r(A, B) = 3$, it would not be unlikely for them misperceive the order of the two landmarks; but when they are outside of this area, i.e. $r(A, B) = (1,\ 5)$, they could be less confident of the observed order as they approach the line connecting the two landmarks.

$$\begin{aligned} f(o)_2 = max(f(o)_2^1,\ f(o)_2^2) &= max(\frac{1}{\sigma_2^1\sqrt{2\pi}}\exp^{-\frac{1}{2}\left(\frac{d(o,PL_a^{AB})}{\sigma_2^1}\right)^2}, \frac{1}{\sigma_2^2\sqrt{2\pi}}\exp^{-\frac{1}{2}\left(\frac{d(o,PL^{AB}{}_{bb})}{\sigma_2^2}\right)^2}) \\ &= \frac{1}{\sigma_2\sqrt{2\pi}}\exp^{-\frac{1}{2}\left(\frac{min(d(o,PL_a^{AB}),d(o,PL_b^{AB}))}{\sigma_2}\right)^2} \end{aligned}$$

where $d(o, PL_a^{AB})$ and $d(o, PL_b^{AB})$ are the distances between viewer o and the two perpendicular lines PL_a^{AB} and PL_b^{AB}, and the standard deviation σ_2^1 and σ_2^2 are assumed equally as σ_2. Note that when two landmarks are very close to each other, such as the example shown in Figure 1(b), viewers may have great uncertainty in deciding where they are located with respect to the two perpendicular lines.

$$f(o)_3 = \frac{1}{\sigma_3\sqrt{2\pi}}\exp^{-\frac{1}{2}\left(\frac{|90^o - o_{ang}|}{\sigma_3}\right)^2} \tag{4}$$

where o_{ang} is the observed angle between A, B from a location o.

Then, the weight of the corresponding change cost of a spatial relation can be defined as being inversely proportional to the probability of individual incorrect perception, as:

$$w_k^r \propto \frac{1}{f(o)_k}, k = 1, 2, 3 \tag{5}$$

E. *Impact of the uncertainty of landmark location*

E.1. Modelling of point landmark uncertainty

The uncertainty of landmark locations could be caused by many reasons in the data capture process [1], such as low accuracy of GPS devices and map digitising. Given the

[1] Cheung, C.K., Shi, W.Z., and Zhou, X., 2004. A probability-based uncertainty model for point-in-polygon analysis in GIS. *GeoInformatica*, 8 (1), 71–98.

coordinates of two landmarks $A(x_1, y_1)$ and $B(x_2, y_2)$, if we model their uncertainty on the X (Easting) and Y (Northing) directions using two independent multivariate Gaussian distributions, and assume the errors on the X and Y directions are uncorrelated, the co-variance matrix of the four location parameters $x_{AB}(x_1, y_1, x_2, y_2)$ can be written as:

$$\mathbf{\Sigma^{A,B}} = \begin{bmatrix} \mathbf{\Sigma^A} & 0 \\ 0 & \mathbf{\Sigma^B} \end{bmatrix} = \left[\begin{array}{cc|cc} \sigma_{x_1}^2 & \sigma_{x_1,y_1} & 0 & 0 \\ \sigma_{x_1,y_1} & \sigma_{y_1}^2 & 0 & 0 \\ \hline 0 & 0 & \sigma_{x_2}^2 & \sigma_{x_2,y_2} \\ 0 & 0 & \sigma_{x_2,y_2} & \sigma_{y_2}^2 \end{array}\right] = \begin{bmatrix} \sigma_{x_1}^2 & 0 & 0 & 0 \\ 0 & \sigma_{y_1}^2 & 0 & 0 \\ 0 & 0 & \sigma_{x_2}^2 & 0 \\ 0 & 0 & 0 & \sigma_{y_2}^2 \end{bmatrix} \tag{6}$$

The values of $(\sigma_{x_1}, \sigma_{y_1})$ and $(\sigma_{x_2}, \sigma_{y_2})$ could be determined based on the sources of data. Assume the uncertain level of landmarks is much smaller than their visibility range, this uncertainty will not affect which landmarks will be observed, but rather how the spatial relations between landmarks will be perceived. As the three types of qualitative spatial relations used in this work are relating to the three types of *Dividing Lines: SL, PL, CL*, we first propagate the uncertainty in landmark locations to these lines.

E.2. Propagating the uncertainty of two co-visible landmarks to their connecting line

Given the coordinates of two landmarks $A(x_1, y_1)$ and $B(x_2, y_2)$, the ***Straight Line*** (SL^{AB}) connecting them can be defined as $\mathbf{Y} = \mathbf{aX} + \mathbf{b}$, where a, b are:

$$\mathbf{a} = \frac{y_2 - y_1}{x_2 - x_1};\ \mathbf{b} = \frac{x_2 * y_1 - x_1 * y_2}{x_2 - x_1} \tag{7}$$

When $x_1 = x_2$, the line equation above can be re-written as $\mathbf{X} = \mathbf{a'Y} + \mathbf{b'}$ where

$$\mathbf{a'} = \frac{x_2 - x_1}{y_2 - y_1};\ \mathbf{b'} = \frac{x_1 y_2 - x_2 y_1}{y_2 - y_1} \tag{8}$$

Then, the uncertainty of landmark locations $\mathbf{\Sigma^{A,B}}$ (as defined in Equation 6) can be propagated to a/a' and b/b' by linearizing the two non-linear functions using first-order Taylor series propagation, written as:

$$\mathbf{\Sigma^{a,b;a',b'}} = \mathbf{J_0 \Sigma^{A,B} J_0^T} \tag{9}$$

where $\mathbf{J_0}$ is the Jacobian matrix containing the first-order partial derivatives of $a,\ b,\ a'\ b'$ on (x_1, y_1, x_2, y_2), calculated as follows:

$$\mathbf{J_0} = \begin{bmatrix} \frac{\partial a}{\partial x_1} & \frac{\partial a}{\partial y_1} & \frac{\partial a}{\partial x_2} & \frac{\partial a}{\partial y_2} \\ \frac{\partial b}{\partial x_1} & \frac{\partial b}{\partial y_1} & \frac{\partial b}{\partial x_2} & \frac{\partial b}{\partial y_2} \\ \frac{\partial a'}{\partial x_1} & \frac{\partial a'}{\partial y_1} & \frac{\partial a'}{\partial x_2} & \frac{\partial a'}{\partial y_2} \\ \frac{\partial b'}{\partial x_1} & \frac{\partial b'}{\partial y_1} & \frac{\partial b'}{\partial x_2} & \frac{\partial b'}{\partial y_2} \end{bmatrix} = \begin{bmatrix} \frac{y_2 - y_1}{(x_2 - x_1)^2} & \frac{-1}{x_2 - x_1} & \frac{y_1 - y_2}{(x_2 - x_1)^2} & \frac{1}{x_2 - x_1} \\ \frac{x_2(y_1 - y_2)}{(x_2 - x_1)^2} & \frac{x_2}{x_2 - x_1} & \frac{x_1(y_2 - y_1)}{(x_2 - x_1)^2} & \frac{-x_1}{x_2 - x_1} \\ \frac{-1}{y_2 - y_1} & \frac{x_2 - x_1}{(y_2 - y_1)^2} & \frac{1}{y_2 - y_1} & \frac{x_1 - x_2}{(y_2 - y_1)^2} \\ \frac{y_2}{y_2 - y_1} & \frac{y_2(x_1 - x_2)}{(y_2 - y_1)^2} & \frac{-y_1}{y_2 - y_1} & \frac{y_1(x_2 - x_1)}{(y_2 - y_1)^2} \end{bmatrix} \tag{10}$$

Then, we can get the uncertainty of a point on the line based on the uncertainty of the slope $\mathbf{a}$, $\mathbf{a'}$ and $\mathbf{b}$, $\mathbf{b'}$ in $\mathbf{\Sigma^{a,b;a',b'}}$. There are three situations:

(1) When $a \neq 0$ and $a' \neq 0$, given a list of X or Y values, we can calculate the corresponding Y or X using $\mathbf{Y} = \mathbf{aX} + \mathbf{b}$ and $\mathbf{X} = \mathbf{a'Y} + \mathbf{b'}$ and the uncertainties on both directions as:

$$\mathbf{\Sigma^{X,Y}} = \begin{bmatrix} \sigma^2_{\mathbf{X}} & \sigma_{\mathbf{X,Y}} \\ \sigma_{\mathbf{X,Y}} & \sigma^2_{\mathbf{Y}} \end{bmatrix} = \mathbf{J_0^2 \Sigma^{a,b;a',b'} J_0^{2T}} \tag{11}$$

where $\mathbf{J_0^2} = \begin{bmatrix} 0 & 0 & Y & 1 \\ X & 1 & 0 & 0 \end{bmatrix}$. If we expand the equation, the error on X and Y directions are equivalent to:

$$\sigma^2_X = \sigma^2_{a'} Y^2 + \sigma^2_{b'} + 2\sigma_{a',b'} X;\ \sigma^2_Y = \sigma^2_a X^2 + \sigma^2_b + 2\sigma_{a,b} X \tag{12}$$

(2) When $a = 0$, the line is horizontal. Therefore, $\sigma^2_X = 0$ and the upper-left part of $\mathbf{\Sigma^{a,b;a',b'}}$ is used to estimate the uncertainty σ^2_Y of points on the Y direction;
(3) When $a' = 0$, the line is vertical. Therefore, $\sigma^2_Y = 0$ and the bottom-right part of $\mathbf{\Sigma^{a,b;a',b'}}$ is used to estimate the uncertainty σ^2_X of points on the X direction.

For example, as shown in Figure B.2, given a landmark $A(0, 0)$ and $B(5, 0)$ with uncertainty $(\sigma_{x_1}, \sigma_{y_1}, \sigma_{x_2}, \sigma_{y_2})$= (0.2, 0.5 0.3 0.8) shown as green and black error ellipses in the 95% and 50% confidence levels, the uncertainty of slope a and intercept b are calculated using Equation 9 as $\mathbf{\Sigma^{a,b}} = \begin{pmatrix} 0.0356 & -0.050 \\ -0.050 & 0.2500 \end{pmatrix}$. The uncertainty of points on the line AB are shown using the upper and lower error bound (red curves) of the line by adding and subtracting the standard deviation of Y at the X of each point.

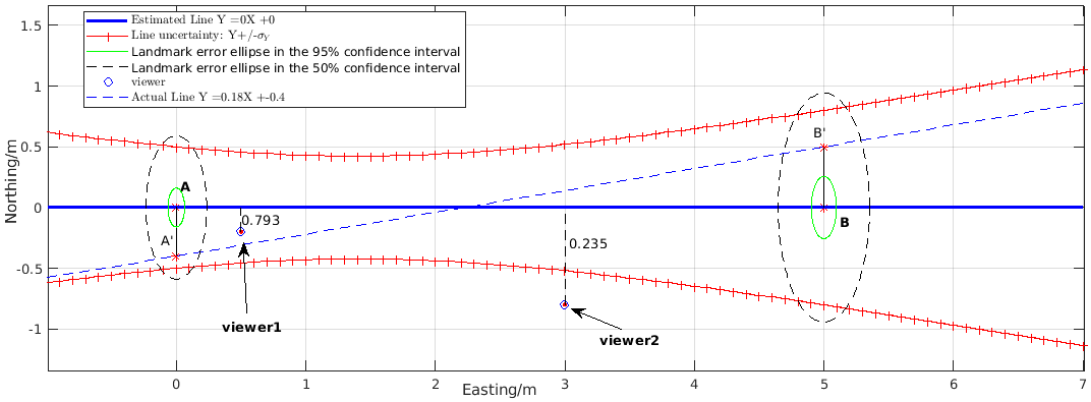

Figure B.2. Propagating the uncertainty of landmark $A(0, 0)$ and $B(5, 0.8)$ to the ***Straight Line*** connecting the two landmarks. Landmark uncertainty is shown as error ellipses while the uncertainty of line SL^{AB} is shown with upper and lower bound red curves. In the areas between the two red curves, a viewer is highly likely to observe an inconsistent ordering relation between the two landmarks.

Probability of a viewer to observe an inconsistent ordering relation between *A* and *B*. Since the location of landmarks A and B are uncertain, it is highly likely that the actual line AB could be anywhere between the upper and lower bound curves. Therefore, the observed ordering relation between A and B could be different from what we expect. For example, as shown in Figure B.2, assume there are two viewers **viewer 1**: $o_1(0.5, -0.2)$ and **viewer 2**: $o_2(3, -0.8)$ located below the solid blue line AB, we would expect both of them to observe A followed by B. However, as the locations

of A, B are actually different from those stored in the map, the actual dividing line is different (shown as a dashed blue line). In this case, although **viewer 2** can still observe A followed by B, **viewer 1** is actually on the other side of the line $SL^{A'B'}$ and would observe B followed by A. Therefore, in the areas between the two red curves, a viewer is highly likely to observe an inconsistent ordering relation.

In fact, depending on the location of a viewer $\mathbf{o}(\mathbf{x_o}, \mathbf{y_o})$ and the uncertainty of the connecting line $\mathbf{\Sigma^{a,b}}$, the likelihood for the viewer to observe a different ordering relation can be estimated by first finding the corresponding point (i.e. nearest point) of the viewer on line SL^{AB} and estimating the corresponding uncertainty of this point $\mathbf{\Sigma^{X_o^1, Y_o^1}}$ using Equation 11.

$$X_o^1 = \frac{ay_o + x_o - ab}{a^2 + 1},\ Y_o^1 = aX_o + b$$

Then, we can approximate the probability $fl(o)_1$ of a viewer being on the straight line, which is considered as their probability to observe an inconsistent ordering relation due to the uncertainty of landmark locations, as follows:

$$fl(o)_1 = \frac{1}{2\pi\sqrt{|\mathbf{\Sigma_{X_o^1, Y_o^1}}|}} \exp^{\left(-\frac{1}{2}(\mathbf{x}-\mu)\mathbf{\Sigma_{X_o^1, Y_o^1}}^{-1}(\mathbf{x}-\mu)^T\right)} \tag{13}$$

where $\mathbf{x}$ is the viewer's location as a two dimensional vector $\mathbf{x} = (x_o\ y_o)$, μ is their corresponding point on the straight line $\mu = [X_o^1\ Y_o^1]$, $\Sigma_{X_o^1, Y_o^1}$ is the covariance matrix of the uncertainty of μ, and $|\Sigma_{X_o^1, Y_o^1}|$ is the determinant of the matrix. Note that when $\Sigma_{X_o^1, Y_o^1}$ is indefinite, Equation 13 can be simplified as by neglecting the interaction terms in the covariance matrix.

For the above example in Figure B.2, the estimated probability of the two viewers observing an inconsistent ordering relation are, respectively, 0.793 and 0.235, which suggests that it is more likely for *viewer 1* to observe an inconsistency than *viewer 2*.
Impact of the distance between two landmarks. For the same example discussed above, if the two landmarks are closer to each other (e.g. $d = 0.2m$) while retaining the same level of uncertainty, the uncertainty of the line will increase rapidly. For example, as shown in Figure B.3, if A keeps still and B moves eastwards from $x_2 = 4m$ to $x_2 = 0.02m$, the slope of line SL^{AB} will increase gradually; the upper and lower error bound will become much sharper, suggesting that from most locations in the space (between the two error bound curves), the observed ordering of the two landmarks will be uncertain.

E.3. Propagating the uncertainty of two co-visible landmarks to perpendicular lines

Similarly, the equations of the two ***Perpendicular Lines*** (PL_a^{AB}, PL_b^{AB}) of line SL^{AB} passing through point A and B can be written as

$$\begin{aligned} &Line\ 1 : \mathbf{Y_1} = \mathbf{a_1 X} + \mathbf{b_1}\ (or\ \mathbf{X_1} = \mathbf{a_1'Y} + \mathbf{b_1'});\\ &Line\ 2 : \mathbf{Y_2} = \mathbf{a_2 X} + \mathbf{b_2}\ (or\ \mathbf{X_2} = \mathbf{a_2'Y} + \mathbf{b_2'}) \end{aligned}$$

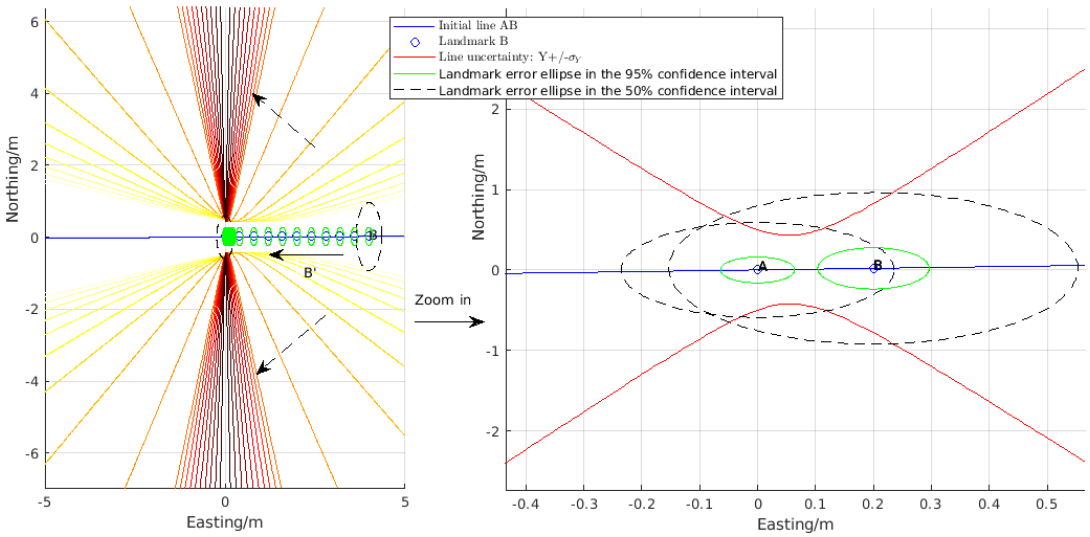

Figure B.3. (Left) When landmark B is getting closer to landmark A, the uncertainty of the straight line AB will increase sharply. The upper and lower bound of the Y values of those lines are shown as coloured curves. (Right) A zoomed view of the error ellipses and error bounds when the distance between A and B equals $0.18m$.

where

$$\mathbf{a_1} = \mathbf{a_2} = \frac{x_1 - x_2}{y_2 - y_1};\ \mathbf{b_1} = y_1 - \frac{x_1 - x_2}{y_2 - y_1}x_1;\ \mathbf{b_2} = y_2 - \frac{x_1 - x_2}{y_2 - y_1}x_2$$
$$\mathbf{a'_1} = \mathbf{a'_2} = \frac{y_1 - y_2}{x_2 - x_1};\ \mathbf{b'_1} = x_1 - \frac{y_1 - y_2}{x_2 - x_1}y_1;\ \mathbf{b'_2} = x_2 - \frac{y_1 - y_2}{x_2 - x_1}y_2$$

Note that $\mathbf{a_1} = \mathbf{a_2}$ and $\mathbf{a'_1} = \mathbf{a'_2}$ as the two perpendicular lines are parallel. Then, we can propagate the landmark uncertainty $\mathbf{\Sigma^{A,B}}$ (in Equation 6) to the parameters of the two perpendicular lines (a_1, b_1, b_2) and (a'_1, b'_1, b'_2), as $\mathbf{\Sigma^{a_1,b_1,b_2;a'_1,b'_1,b'_2}} = \mathbf{J_1 \Sigma^{A,B} J_1^T}$, where $\mathbf{J_1}$ is the Jacobian matrix calculated as below:

$$\mathbf{J_1} = \begin{bmatrix} \frac{\partial a_1}{\partial(x_1,y_1,x_2,y_2)} \\ \frac{\partial b_1}{\partial x_1,y_1,x_2,y_2)} \\ \frac{\partial b_2}{\partial x_1,y_1,x_2,y_2)} \\ \frac{\partial a'_1}{\partial(x_1,y_1,x_2,y_2)} \\ \frac{\partial b'_1}{\partial x_1,y_1,x_2,y_2)} \\ \frac{\partial b'_2}{\partial x_1,y_1,x_2,y_2)} \end{bmatrix} = \begin{bmatrix} \frac{1}{y_2-y_1} & \frac{x_1-x_2}{(y_2-y_1)^2} & \frac{-1}{y_2-y_1} & \frac{x_2-x_1}{(y_2-y_1)^2} \\ \frac{-2x_1+x_2}{y_2-y_1} & [1 - \frac{x_1(x_1-x_2)}{(y_2-y_1)^2}] & \frac{x_1}{y_2-y_1} & \frac{x_1(x_1-x_2)}{(y_2-y_1)^2} \\ \frac{-x_2}{y_2-y_1} & \frac{-x_2(x_1-x_2)}{(y_2-y_1)^2} & \frac{2x_2-x_1}{y_2-y_1} & [1 + \frac{x_2(x_1-x_2)}{(y_2-y_1)^2}] \\ \hline \frac{y_1-y_2}{(x_2-x_1)^2} & \frac{1}{x_2-x_1} & \frac{y_2-y_1}{(x_2-x_1)^2} & \frac{-1}{x_2-x_1} \\ 1 - \frac{y_1(y_1-y_2)}{(x_2-x_1)^2} & \frac{-2y_1+y_2}{x_2-x_1} & \frac{y_1(y_1-y_2)}{(x_2-x_1)^2} & \frac{y_1}{x_2-x_1} \\ \frac{-y_2(y_1-y_2)}{(x_2-x_1)^2} & \frac{-y_2}{x_2-x_1} & 1 + \frac{y_2(y_1-y_2)}{(x_2-x_1)^2} & \frac{2y_2-y_1}{x_2-x_1} \end{bmatrix} \tag{14}$$

Then, given a list of points on the line as (X, Y), the errors of Y_1 and Y_2 are:

(1) When $a_1 \neq 0$ and $a'_1 \neq 0$, the two perpendicular lines are neither vertical nor horizontal, the uncertainty of a point on these lines can be estimated by:

$$\mathbf{\Sigma^{X_1,Y_1}} = \begin{bmatrix} \sigma^2_{\mathbf{X_1}} & \sigma_{\mathbf{X_1},\mathbf{Y_1}} \\ \sigma_{\mathbf{X_1},\mathbf{Y_1}} & \sigma^2_{\mathbf{Y_1}} \end{bmatrix} = \mathbf{J_2 \Sigma^{a_1,b_1,b_2;a'_1,b'_1,b'_2} J_2^T} \tag{15}$$

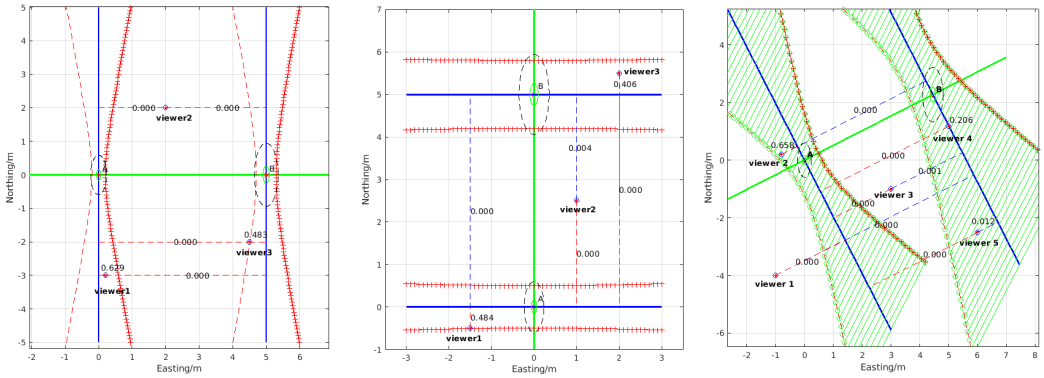

(a) Landmarks A and B are on a horizontal line.

(b) Landmarks A and B are on a vertical line.

(c) Landmarks A and B are neither horizontal nor vertical.

Figure B.4. The uncertainty of the perpendicular lines of line AB as well as the probabilities of viewers to be on such lines, which are considered as their probability to observe an inconsistent relative orientation relation from those locations.

where $\mathbf{J_2} = \begin{bmatrix} 0 & 0 & 0 & Y_1 & 1 & 0 \\ X_1 & 1 & 0 & 0 & 0 & 0 \end{bmatrix}$. If we expand the equation, the error on X and Y directions are equivalent to:

$$\begin{array}{l|l} \sigma^2_{X_1} = \sigma^2_{a'_1} Y^2 + \sigma^2_{b'_1} + 2\sigma_{a'_1,b'_1} X; & \sigma^2_{X_2} = \sigma^2_{a'_1} Y^2 + \sigma^2_{b'_2} + 2\sigma_{a'_1,b'_2} X \\ \sigma^2_{Y_1} = \sigma^2_{a_1} X^2 + \sigma^2_{b_1} + 2\sigma_{a_1,b_1} X; & \sigma^2_{Y_2} = \sigma^2_{a_1} X^2 + \sigma^2_{b_2} + 2\sigma_{a_1,b_2} X \end{array}$$

(2) When $a_1 = 0$, $a'_1 = Inf$, the two perpendicular lines are horizontal. Therefore, $\sigma^2_{X_1} = \sigma^2_{X_2} = 0$ and the upper-left part of $\mathbf{\Sigma^{a_1,b_1,b_2;a'_1,b'_1,b'_2}}$ is used to estimate the uncertainty of points on the lines on the Y direction as: $\sigma^2_{Y_1}$ and $\sigma^2_{Y_2}$.

(3) When $a'_1 = 0$, $a_1 = Inf$, the two perpendicular lines are vertical. Therefore, $\sigma^2_{Y_1} = \sigma^2_{Y_2} = 0$ and the bottom-right part of $\mathbf{\Sigma^{a_1,b_1,b_2;a'_1,b'_1,b'_2}}$ is used to estimate the uncertainty of points on the lines on the X direction as $\sigma^2_{X_1}$ and $\sigma^2_{X_2}$.

Three examples are shown in Figure B.4 to illustrate the above three scenarios. Given the location of a viewer $o(x_o, y_o)$, we first find their nearest points on the two perpendicular lines PL^{AB}_a and PL^{AB}_b as

$$X^{2,i}_o = \frac{a_1 y_o + x_o - a_1 b_i}{a_1 a_1 + 1},\ Y^{2,i}_o = a_1 X^{2,i}_o + b_i$$

where $i = 1, 2$. Then, the corresponding uncertainty of the two points $\mathbf{\Sigma^{X^{2,i}_o, Y^{2,i}_o}}$ and the probability $fl(o)^i_2$ of a viewer being on each perpendicular line can be calculated using Equation 15 and Equation 13. For example, in the scenario shown in Figure B.4 (a), the estimated probability for the three viewers being potentially on the two perpendicular lines are respectively $fl(o_1)_2 = (0.629,\ 0.000)$, $fl(o_2)_2 = (0.000,\ 0.000)$ and $fl(o_3)_2 = 0.000,\ 0.483$. The higher of the two probabilities is considered as the viewer's probability to observe a different relative orientation relation compared to those pre-calculated ones in the reference database. Therefore, it is likely for *viewer 1* to observe an index 1 rather than 3, but it is very unlikely for *viewer 2* to misjudge a relative orientation index other than 3.

E.4. Propagating the uncertainty of two co-visible landmarks to their circular line

In order to propagate the location uncertainty of landmarks A and B onto the corresponding ***Circular Line*** (CL^AB), the equation of points P on the half-circle passing through point A and B are written as:

$$\begin{aligned} \mathbf{X} &= (\mathbf{x_2} - \mathbf{x_1})\mathbf{cos}(\phi)^\mathbf{2} + (\mathbf{y_2} - \mathbf{y_1})\mathbf{sin}(\phi)\mathbf{cos}(\phi) \\ \mathbf{Y} &= (\mathbf{y_2} - \mathbf{y_1})\mathbf{cos}(\phi)^\mathbf{2} - (\mathbf{x_2} - \mathbf{x_1})\mathbf{sin}(\phi)\mathbf{cos}(\phi) \end{aligned} \tag{16}$$

where ϕ is the clockwise angle of vector $\overrightarrow{AP}$ with respect to $\overrightarrow{AB}$, as shown in Figure B.5 (a). When $\phi \in [0,\ \frac{\pi}{2}]$, the points are on the bottom half of the circle from where A would be observed before B; when $\phi \in (\frac{\pi}{2},\ \pi]$, the points are on the top part of the circle from where B would be observed before A.

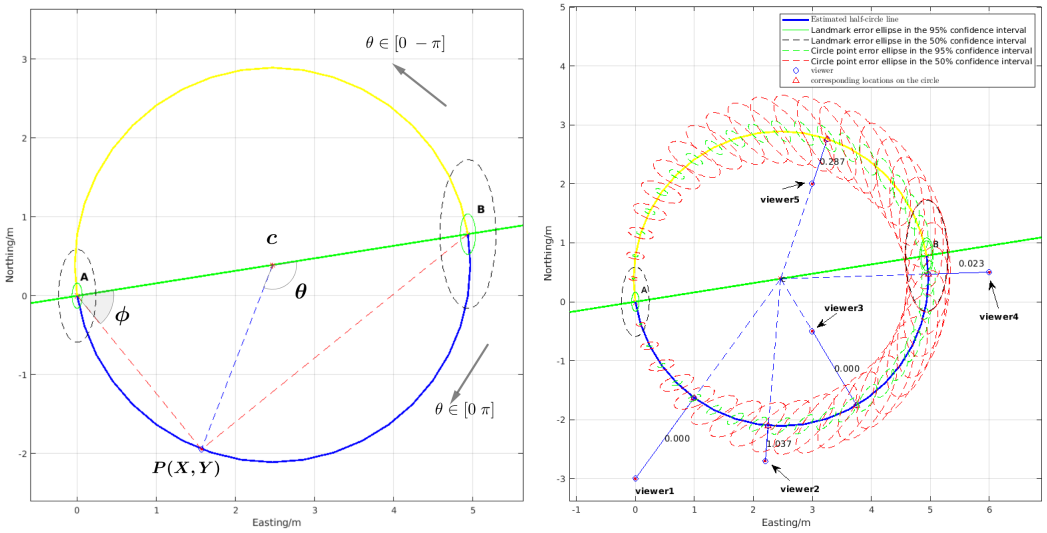

(a) Definition of θ and ϕ.

(b) Uncertainty of points on the circle.

Figure B.5. a) Definition of a circle with a diameter AB; b) Uncertainty of points on the circle are defined by the uncertainty of landmarks A and B and the probabilities of viewers being on the circle.

Then, given a ϕ, the location uncertainty of a point on the circle can be estimated by propagating the uncertainty of the landmark pair $\mathbf{\Sigma^{A,B}}$ as in previous sections, written as: $\mathbf{\Sigma^{X,Y}} = \begin{bmatrix} \sigma_\mathbf{X}^\mathbf{2} & \sigma_{\mathbf{X,Y}} \\ \sigma_{\mathbf{X,Y}} & \sigma_\mathbf{Y}^\mathbf{2} \end{bmatrix} = \mathbf{J_3}\mathbf{\Sigma^{A,B}}\mathbf{J_3^T}$, where $\mathbf{J_3}$ is the Jacobian matrix calculated as below:

$$\mathbf{J_3} = \begin{bmatrix} \frac{\partial X}{\partial(x_1,y_1,x_2,y_2)} \\ \frac{\partial Y}{\partial x_1,y_1,x_2,y_2)} \end{bmatrix} = \begin{bmatrix} -cos(\phi)^2 & -sin(\phi)cos(\phi) & cos(\phi)^2 & sin(\phi)cos(\phi) \\ sin(\phi)cos(\phi) & -cos(\phi)^2 & -sin(\phi)cos(\phi) & cos(\phi)^2 \end{bmatrix} \tag{17}$$

Since the location of the circle is uncertain, the actual angle observed between A and B could change between *obtuse* and *acute*. To estimate the probability of a viewer $\mathbf{o}(\mathbf{x_o}, \mathbf{y_o})$ to observe a different qualitative angle to the stored one, we first need to find its corresponding point P on the circle, which is the intersection of the circle with the line connecting the circle centre $c(\frac{x_1+x_2}{2}\ \ \frac{y_1+y_2}{2})$) and the viewer o, as shown in

Figure B.5 (b). To do this, the angle ϕ_o^3 from the vector $\overrightarrow{AB}$ to $\overrightarrow{AP}$ is calculated as:

$$\begin{aligned} & v_1 = \overrightarrow{cB} = [x_2\ y_2] - c;\ v_2 = \overrightarrow{co} = [x_o\ y_o] - c; \\ \Rightarrow\ & \theta_o^3 = -atan2(v_1^1 v_2^2 - v_1^2 v_2^1, v_1^1 v_2^1 + v_1^2 v_2^2) \\ \Rightarrow\ & \phi_o^3 = \theta_o^3/2 \end{aligned} \tag{18}$$

Then, the coordinates of the intersection point $(\mathbf{X_o^3}, \mathbf{Y_o^3})$, its associated uncertainty $\mathbf{\Sigma^{X_o^3, Y_o^3}}$, and the probability $fl(o)_3$ of a viewer being on the circle can be estimated by propagating the uncertainty of landmarks as in Equation 13. $fl(o)_3$ is also considered as the viewer's probability to encounter an inconsistent qualitative angle between A and B. For example, with the two landmarks $A(0, 0)$ and $B(4.94, 0.78)$ shown in Figure B.5 (b) with uncertainty $(\sigma_{x_1}, \sigma_{y_1}, \sigma_{x_2}, \sigma_{y_2})$= (0.2, 0.5 0.3 0.8), the estimated probability for the five viewers to potentially be on the circular lines are respectively $fl(o)_3 = (0.000, 1.037, 0.000, 0.023, 0.287)$, suggesting that Viewer 5 is most likely to observe an obtuse angle rather than the expected acute one.

E.5. Propagating the uncertainty of a landmark to its Boundary Line

As mentioned earlier in Section 2 of the main manuscript, the visibility range of a landmark is first defined as a simplified circular (or fan-shaped) buffer zone with a certain radius, then clipped by the outlines of buildings using a 2D viewshed algorithm (see Algorithm 1 in Section C). Therefore, the ***Boundary Line (BL)*** of a landmark A can either be on a circle or on building facades. An example is given below in Figure B.6.

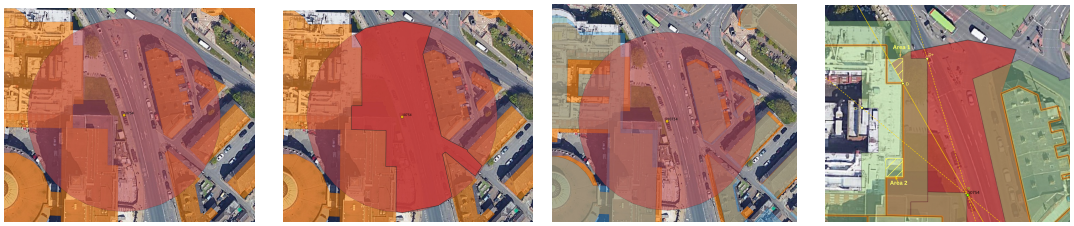

(a) (b) (c) (d)

Figure B.6. In these figures, (a-b) orange polygons represent the buildings extracted from the OpenStreetMap, the light red area demonstrates the visibility range of a landmark, and the dark red area in the right image shows the visibility range after considering the occlusion by buildings. (c) Incoherent building outlines are observed in OpenStreetMap (orange), Ordnance Survey (blue) and Google Satellite Image. (d) The uncertainty of building outlines can be shown as a buffer zone of the building outlines. The orange lines are the outlines of buildings (OSM) and the light green zones are the 8-metre buffer zones of the building outlines.

- When a viewer is very close to the circular boundary (i.e. away from the landmark centre), they may not be able to observe the landmark as expected due to the location uncertainty of the landmark. Location of the points on the circular range boundary of the landmark (x_1, y_1) written as: $(X = x_1 + Rcos(\theta);\ Y = y_1 + Rsin(\theta))$, where $\theta \in [0\ 2\pi]$ (when there is no occlusion). It can be seen from the above equations that the uncertainty of these points is simply the same as the centre landmarks: $\mathbf{\Sigma^{X_4, Y_4}} = \mathbf{\Sigma^{A,B}}$. Given the location of a viewer $o(x_o, y_o)$, if their situated place cell is on the circular boundary, the nearest point of the

viewer on the boundary can be identified by:

$$X_o^4 = \frac{R(x_o - x_1)}{\sqrt{(x_o - x_1)^2 + (y_o - y_1)^2}} + x_1;\ Y_o^4 = \sqrt{R^2 - (X_o^4 - x_1)^2} + y_1 \tag{19}$$

Then, the probability $fl(o)_4$ of a viewer being on the circle, i.e. the probability of a viewer to miss the landmark due to the landmark location uncertainty, can be approximated as in Equation 13.

- When the visibility boundary is on building facades, the situation becomes a bit more complex. For example, offsets were observed in the building maps from OpenStreetMap (orange areas), Ordnance survey (blue areas) and Google Satellite Image, as shown in Figure B.6(c).

These offsets bring in two types of uncertainty in generating the place cells and place signatures. Specifically,

(1) when the outline of a building is actually further away from a landmark than expected (based on an existing map), some free space with a clear view to the landmark could be missing from the pre-defined place cells, such as **Area 2** in the Figure B.6 (d). Therefore, if a viewer is in one of these areas, no exactly matched place signature would be found in the reference database;
(2) when the actual outline of a building is closer to the landmark than expected, this landmark is in fact invisible in some areas in the pre-generated place cells, such as **Area 1** in the Figure B.6 (d).

For the second type of uncertainty, we can propagate the uncertainty from building outlines to place cells based on their distances to buildings, using the similar procedure as in Section E.2 and Section E.3. However, as seen in Figure B.6 (d), offsets in different scales and directions could be observed for different buildings, making it difficult to assign a general error level. Ideally, a local alignment would be ideal to remove these offsets. To not increase the length of this article further, this task is left for future work.

References

Schlieder, C., 1993. Representing visible locations for qualitative navigation. *Qualitative Reasoning and Decision Technologies*, 523–532.